JOURNAL OF MATERIALS SCIENCE 31 (1996) 4907–4911

The effect of post-heat treatment of laser surface melted AISI 1018 steel

A. S. AKKURT
Arçelik A. Ş., Research Development Center, Tuzla 81719, Istanbul, Turkey
O. V. AKGÜN
University of Istanbul, Department of Metallurgical Engineering, Avcilar, Istanbul, Turkey
N. YAKUPOĞLU
Istanbul Technical University, Department of Metallurgical Engineering, Maslak, Istanbul, Turkey

The effect of laser surface melting (LSM) and following heat treatment on the microstructure of AISI 1018 steel was investigated. The microstructures of the samples (as-received, laser treated, and heat treated) were characterized using optical microscopy, scanning electron microscopy with energy-dispersive spectrometry, and hardness testing techniques. The post-heat treatment of laser-treated samples was carried out at 900°C for 10 min followed by quenching universe water and oil. As the quenching rate decreased, the hardness of the melted layers decreased significantly, although the grain size of the melted region was still very small compared to the unaffected material. This was due to the very small austenite grain size which offered more grain-boundary area where decomposition can nucleate. Heavy Mn–Si precipitates were observed in the laser-treated layers, and post-heat treatment resulted in increased diameters of these particles owing to the lengthy time for diffusion.

1. Introduction

Laser surface modification, such as heating and melting, has become a novel technique which is applied to metals and alloys. Laser-treatment of a thin surface layer, followed rapid self-quenching, increases several properties, such as hardness, abrasion and corrosion resistance, of alloys. This process also helps in dissolving precipitated and segregated phases, and finely redistributing inclusions and impurities. In the laser surface process, increase in hardness can be achieved by either phase transformations, e.g. martensite formation in carbon steels, or refinement of subgrain structure, or both.

There is an increasing interest in applying the laser surface melting process to stainless steels [1, 2], tool steels [3, 4], and ferrous and non-ferrous alloys [5–10]. In this investigation, the effect of laser surface melting on microstructure and hardness of AISI 1018 steel was studied. Heat treatments were carried out to introduce microstructural changes in the melted zone and to determine their effects on the hardness of the melted and heat-affected zone. Although the laser treatment of a low-carbon steel may not have any commercial significance, it is interesting to observe and show the effect of the heat treatment on laser-treated regions and to relate it to other materials.

2. Experimental procedure

The material used in this study was a commercial grade AISI 1018 steel bar of 12 mm thickness. As-received alloy was cut and ground flat to 600 grid for laser processing.

Laser surface melting experiments were carried out in a nitrogen gas atmosphere and a GTE Sylvania Model 975 CO_2 gas transport laser, which has a nominal output power of 5 kW, was used. No coating was applied, to avoid any surface contamination of the samples. The specimens were mounted on a rotating table, swept through the beam focused on the surface. The beam diameter at the laser exit aperture was 47.5 mm and could be focused down to 0.5 mm through a focusing lens. Approximately 9 cm^2 surface area was melted with 50% overlap.

Vickers' microhardness of the laser-treated samples was measured using a Shimadzu HMV-2000 Microhardness Tester with an applied load of 200 g for 10 s.

Microstructural characterizations were conducted using optical and scanning electron microscopy (SEM) with energy dispersive spectrometry (EDS) (Jeol JSM-6400 and Tracor VOYAGER 2110, respectively). For optical and scanning electron microscopy, the samples were sectioned, polished and etched in 2% Nital solution.

0022–2461

Laser-treated samples with untreated substrate were homogenized at 900 °C and quenched in water and oil. The samples of laser surface melted, heat-treated laser surface melted quenched in water, and heat-treated laser surface melted quenched in oil, are denoted LSM 1018, HTWQ-LSM 1018, and HTOQ-LSM 1018, respectively.

3. Results and discussion

3.1. LSM 1018 sample

Using an optical microscope, it is possible to observe the shape of the laser-melted zone and to measure its diameter, which is about 500 μm. Observation of the longitudinal cross-section of the as-laser-processed samples showed that there are three different zones in the microstructure: (a) unaffected matrix material, (b) melted region, and (c) heat-affected zone.

3.1.1. Unaffected material and melted zone

The microstructure of the as-received AISI 1018 steel and the unaffected material after laser processing, consists of ferrite and pearlite phases oriented in the rolling direction showing a classical low-carbon steel structure. To obtain a large surface area to be melted on the material surface, a series of successive passes with 50% overlap melting was performed vertical to the rolling direction. Owing to the overlap melting, a mixed microstructure of martensite, bainite, and pearlite was formed in the melted zone, which is shown by optical micrography together with HAZ and the unaffected region in Fig. 1. The variation in the hardness values taken horizontally from the cross-section of the treated surface, confirms the presence of these different phases (Fig. 2). This also indicates that the laser melting process with successive passes does not produce a homogeneous surface structure. EDS analysis of manganese and silicon elements from the melted and matrix material showed that there is no loss of these elements during laser melting.

During multiple melting, some part of the first melted region is remelted, thus, the remaining part becomes the heat-affected zone (HAZ) of the second melted zone. In some part of the HAZ, temperature during melting exceeds the austenitization temperature resulting in solid-state transformations; therefore, in this region, hardness values decrease compared to the regions where temperatures are lower than the austenitization temperature. The microstructure of this area (A in Fig. 1b) is composed of fine bainite. In the other part of the HAZ where temperatures are lower (B), tempered martensite structure is observed. These hardness values showed a gradual increase towards the next overlapped boundary (A). The cycling of the hardness ends up at the last pass, where, VHN hardness values as high as 710 are recorded. Because this last pass does not undergo tempering, the very fine martensitic microstructure, formed due to laser melting and rapid self-quenching, remains unchanged, thus giving high hardness values, as expected from the martensitic structure. The vertical hardness profile taken only from the unoverlapped regions, showed reasonably uniform distribution that implies the presence of a less-mixed microstructure. However, significant variation in the hardness values was observed when the vertical hardness profile includes the overlapped regions (A) where the hardness values are the lowest in the overall melted region.

Figure 1 (a) Cross-section of LSM 1018 showing the different regions; and (b) schematic representation of (a); (a) is taken from the oblong area in (b).

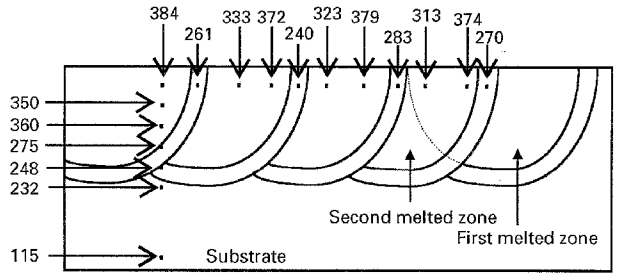

Figure 2 Variation in the hardness values in the cross-section of an LSM 1018 sample.

Another beneficial effect of laser melting is the removal and/or fine redistribution of inclusions and impurities that could be present in materials. In our case, elongated MnS inclusions are not seen but are very finely distributed in the melted region due to laser melting and the high cooling rate.

3.1.2. Heat-affected zone

Fig. 1 shows the melted region, HAZ in the substrate (C), and the unaffected region. The temperature outside the melted region decreases from the boundary between the melted and unmelted region toward the substrate. Higher temperatures, which are less than the melting temperature of the alloy, affect the nearby structure. In our case, only the dissolution of pearlitic structure close to the melted region was observed (C). As seen in Fig. 3, the cementite dissolution decreases as the temperature effect becomes less pronounced. The regions very close to the melted zone, i.e., 100 μm (Fig. 3a), constituted of ferrite and carbide, cannot be distinguished owing to the significant effect of higher temperatures. However, as the distance from the melted region increases, i.e. 335 μm (Fig. 3c), there is no observable dissolution in the pearlitic structure.

3.2. Heat-treated LSM 1018 sample

3.2.1. HTWQ-LSM 1018 sample

The microstructure of the HTWQ-LSM 1018 sample homogenized at 900 °C and subsequently water quenched was very fine ferrite and pearlite in the melted zone (Fig. 4a). In this case, the grain size of the melted zone is more observable, between 5 and 10 μm, compared to that of as-lasered sample. The pearlitic structure can be seen only at high magnifications, e.g. × 5000 (Fig. 4b). This structure greatly differs from the substrate which was exposed to the same heat treatment, and resulted in a mainly martensite microstructure (Fig. 4c). This discrepancy in microstructure can be explained in terms of austenite decomposition rate. Austenite decomposition rate can be controlled in two ways: austenite grain size and alloy retardation; although time is also very effective, it is not important in our case because both regions experienced the same heat treatment. Alloy retardation also cannot be a factor in our material because both regions share the same bulk and there was virtually no elemental loss in the laser-melted region. In the melted region, austenite grain size was very small compared to that of the

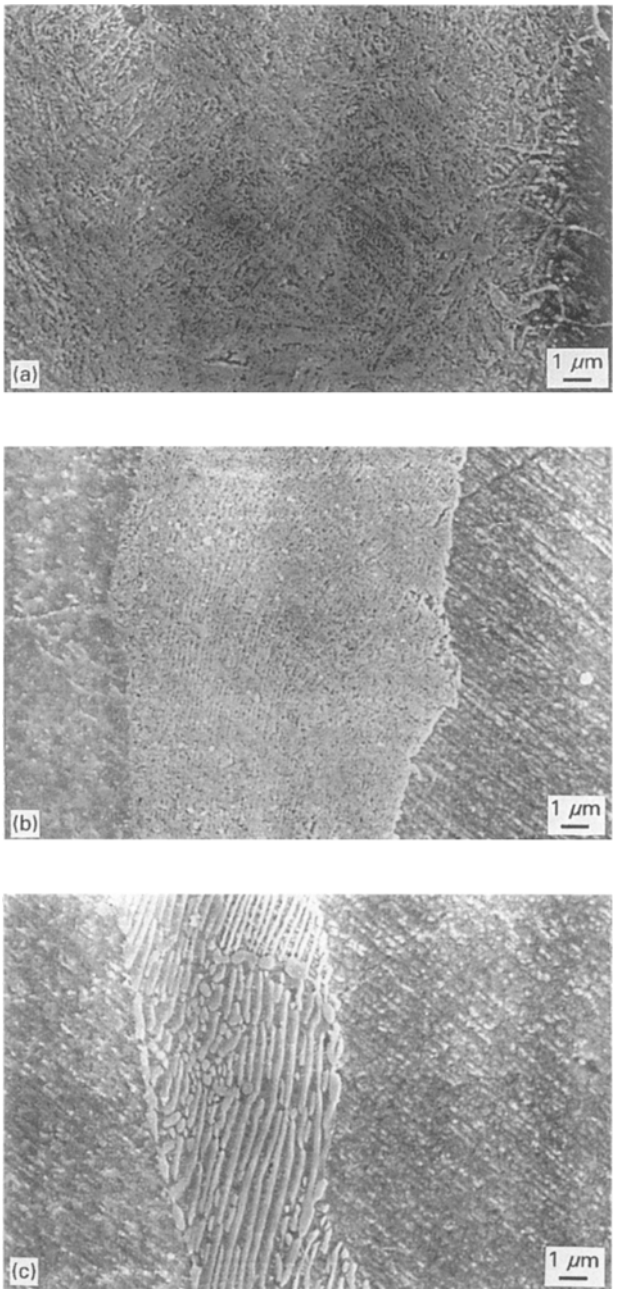

Figure 3 Scanning electron micrographs showing the effect of temperature on the dissolution of pearlitic structure. The temperature effect decreases through (a), (b) and (c).

substrate (almost five-fold). Because a finer grain size offers a greater grain-boundary area per unit volume than a coarser grain size, there will be a higher rate of the decomposition of austenite to ferrite and pearlite. On the other hand, owing to the large initial austenite grain size, the rate of decomposition will be very slow or the reaction cannot be initiated, resulting in a martensitic structure.

The microstructural observations are also consistent with the hardness values measured in both regions (Fig. 5). Hardness values in the melted region are fairly uniform and almost half those of the substrate.

3.2.2. HTOQ-LSM 1018 sample

The effect of smaller austenite grain size on the decomposition of the austenite becomes very significant

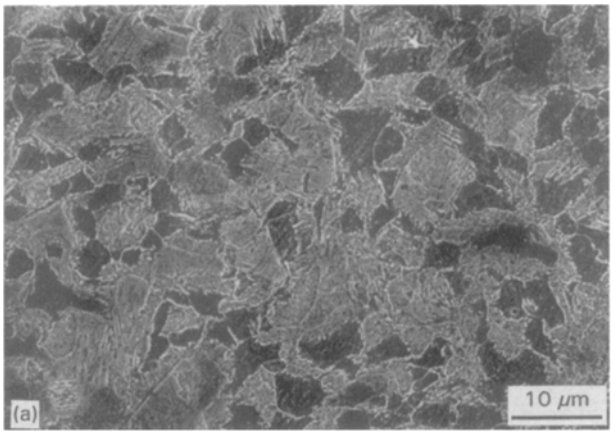

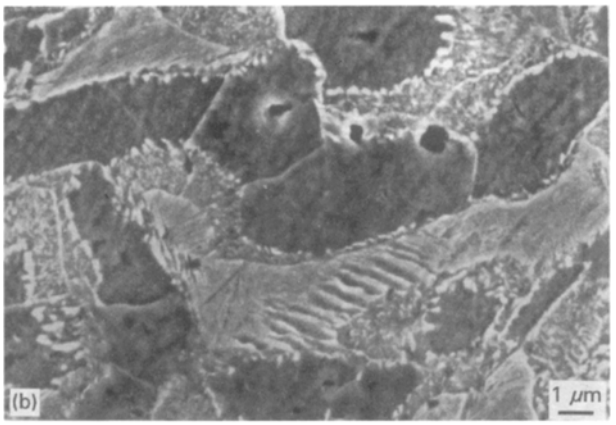

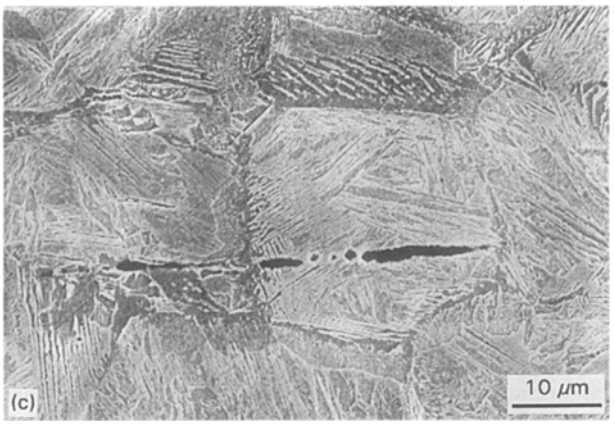

Figure 4 (a) The microstructure of HTWQ-LSM 1018 (b) higher magnification view of the same area, and (c) the microstructure of unmelted matrix material after water quenching.

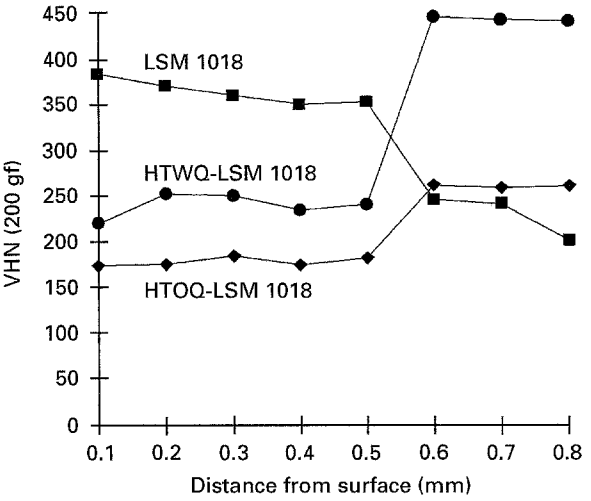

Figure 5 Hardness values of (■) LSM 1018, (●) HTWQ-LSM 1018, and (◆) HTOQ-LSM 1018 samples as a function of distance from the surface.

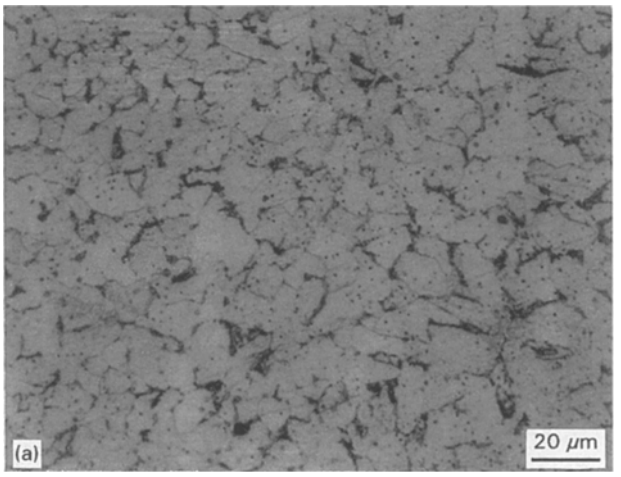

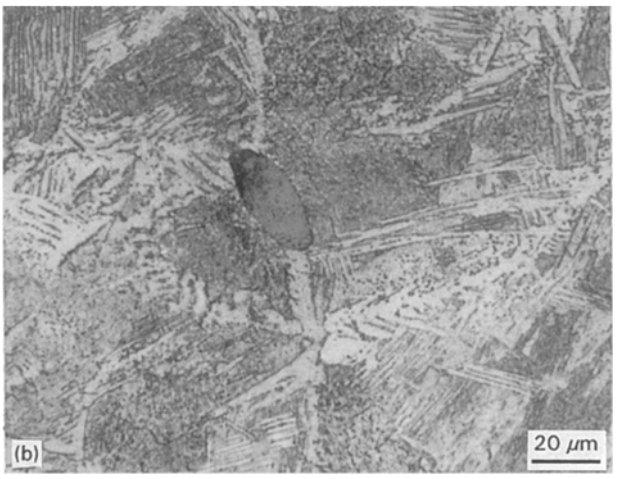

Figure 6 The microstructures of (a) melted and (b) matrix material after oil quenching.

for the homogenized then oil-quenched samples. Decomposition of austenite in the melted region occurred very quickly in the cooling rate used. After that, the products had more time to grow than that of water-quenched material, thus, the hardness decreased further. As seen in Fig. 6, the decomposition products are ferrite and carbide, and carbides form discontinuously around the ferrite grains. In the substrate, the microstructure consists of pearlite and a small amount of ferrite, which outlines the prior austenite grain boundaries. Some Widmanstätten ferrites can also be seen in the microstructure.

Another feature in the microstructure of the melted region is the observable spherical Mn–Si compounds formed due to the lengthy diffusion time (Fig. 7). These particles were identified by EDS. Although Mn–Si particles also existed in LSM 1018 and HTWQ-LSM 1018 samples, they were not big enough to be seen at magnifications as high as $\times 5000$. Mn–Si spheres in the HTOQ-LSM 1018 sample had a diameter of approximately 3 μm at maximum, and less. The distance between large spheres was measured to be nearly 75 μm.

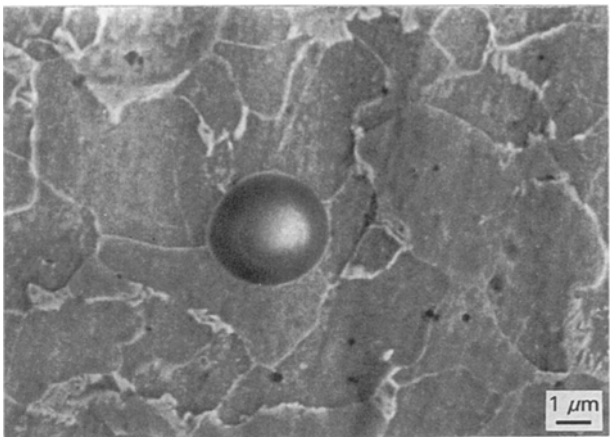

Figure 7 Scanning electron micrograph of a Mn–Si particle in the melted region after oil quenching.

The mean hardness value in the melted region was about 175 VHN, which is higher than the value expected from a microstructure consisting of ferrite and carbide. This indicates the contribution of smaller grain size to the hardness. Hardness values taken from the substrate, which have a mean value of 250 VHN, are consistent with the observed microstructure.

4. Conclusions

This study has attempted to show the effect of post-heat treatment on laser-melted surface of 1018 steel, but the conclusions can be applied to other carbon steels. The following conclusions can be drawn.

1. The surface hardness of 1018 steel can be significantly increased by laser surface melting by the formation of martensitic and fine grain-size structure. However, owing to the tempering effect by overlapping of successive laser passes, the martensitic structure decomposed to tempered martensite, resulting in lower hardness values. For example, while VHN values as high as 710 were recorded in the last pass which was not overlapped, the overlapped melted regions showed VHN values only between 260 and 380.

2. Post-heat treatment changed significantly the microstructural properties. Owing to the very small austenite grain size of the melted region, austenite decomposition was easily completed upon quenching and resulted in low hardness values. In the case of oil quenching, there was also sufficient time for decomposition products, ferrite and pearlite, which resulted in lower hardness values than those of water-quenched samples.

3. Mn–Si precipitates were observable only in oil-quenched conditions. EDS analysis showed no loss of manganese nor silicon due to laser melting. Elongated MnS inclusions present in the unaffected material were not seen, but were very finely distributed in the melted region owing to laser melting and the high cooling rate.

4. The dissolution of pearlitic structure close to the melted region was observed. The cementite dissolution decreased as the temperature effect became less pronounced. The regions very close to the melted zone, constituted of ferrite and carbide, could not be distinguished owing to the significant effect of higher temperatures. However, as the distance from the melted region increased there was no observable dissolution in the pearlitic structure.

References

1. P. A. MOLIAN and W. E. WOOD, *J. Mater. Sci.* **18** (1983) 2555.
2. O. V. AKGÜN and O. T. INAL, *ibid.* **29** (1994) 1159.
3. H. BANDE, G. L. L'ESPÉRANCE, M. U. ISLAM and A. K. KOUL, *Mater. Sci. Technol.* **7** (1991) 452.
4. P. R. STRUTT, *Mater. Sci. Eng.* **44** (1980) 239.
5. J. R. BRADLEY and S. KIM, *Metall. Trans.* **19A** (1988) 2013.
6. M. R. FISHMAN and J. ZAHAVI, *J. Mater. Sci.* **23** (1988) 1547.
7. J. M. PELLETIER, D. PERGUE, F. FOUQUET and H. MAZILLE, *ibid.* **24** (1989) 4343.
8. S. KATAYAMA, A. MATSUNAWA, A. MARIMOTO, S. ISHIMOTO and Y. ARATA, in "Laser Processing of Materials", edited by K. Mukherjee and J. Mazumder (AIME, New York, 1985) p. 159.
9. J. D. AYERS, in "Lasers in Metallurgy", edited by K. Mukherjee and J. Mazumder (AIME, New York, 1981) p. 115.
10. Y. W. KIM, P. R. STRUTT and H. NOWOTONY, *Metall. Trans.* **10A** (1979) 881.

Received 1 December 1994
and accepted 4 October 1995